J. Fluid Mech. (1976), *vol.* 75, *part* 4, *pp.* 647–656
Printed in Great Britain

The phase configuration of waves around a body moving in a rotating stratified fluid

By K. S. PEAT AND T. N. STEVENSON
Department of the Mechanics of Fluids, University of Manchester, England

(Received 16 February 1976)

A body is started impulsively from rest and moves on an arbitrary path in an incompressible, stably stratified, rotating fluid. The phase configuration of the waves which are generated is studied using small amplitude wave theory. The theory is compared with experiment for a few special cases which include a horizontal cylinder (*a*) oscillating about a position fixed in the fluid, (*b*) moving with constant velocity and (*c*) moving with a constant angular velocity in a circular path relative to the fluid. Theory and experiment show reasonable agreement except where wakes interfere with the wave pattern.

1. Introduction

The phase configuration of the inviscid incompressible internal waves which develop around a body moving in a stably stratified fluid which has a constant buoyancy frequency has been discussed by Görtler (1943), Lighthill (1967), Mowbray & Rarity (1967), Rarity (1967), Stevenson (1969, 1973) and Stevenson & Thomas (1969). The phase configuration of inertial waves generated by a body moving in a steadily rotating fluid have been described by Görtler (1944, 1957), Oser (1958), Nigam & Nigam (1962), Lighthill (1967) and Prabhakara Rao (1973). In many geophysical phenomena, fluid is both rotating and stratified. Subba Rao & Prabhakara Rao (1971) have considered such a fluid and have calculated the axisymmetric waves around a body moving along the axis of rotation, and Redekopp (1975) has considered both two- and three-dimensional bodies moving with a constant mean velocity in a horizontal plane.

The theoretical work is now extended to the waves around a point body and a two-dimensional body which move on an arbitrary path in a rotating stratified fluid. Small amplitude wave theory is used to obtain an equation for the far-field phase configuration of the waves in terms of a body velocity which can vary with time. The equation is used to find the wave system around a horizontal cylinder which (*a*) oscillates, (*b*) moves with constant velocity at various angles to the horizontal, (*c*) oscillates and moves with a constant mean velocity in a horizontal plane, (*d*) moves with constant angular velocity on a circular path in a vertical plane and (*e*) oscillates and moves on a circular path. For cases (*a*), (*b*) and (*d*) the theory is compared with experiments in which the wave systems are observed with a schlieren system. The theory for the Cauchy–Poisson waves due to an impulsive start is included but, unlike the situation in purely stratified flow (Stevenson 1973), their presence in the experiments is scarcely visible.

2. Analysis

For an inviscid, incompressible, non-diffusive flow of a rotating stratified fluid, the equations of motion written with respect to a co-ordinate system rotating with the fluid are (Greenspan 1968, p. 5)

$$\nabla . \mathbf{q} = 0, \quad D\rho/Dt = 0 \tag{1), (2}$$

and
$$\rho[\partial \mathbf{q}/\partial t + \tfrac{1}{2}\nabla(\mathbf{q}.\mathbf{q}) + (\nabla \wedge \mathbf{q}) \wedge \mathbf{q} + 2\Omega \wedge \mathbf{q}] = -\nabla P - \rho \mathbf{\Omega} \wedge (\mathbf{\Omega} \wedge \mathbf{r}) - \rho g \mathbf{k}, \tag{3}$$

where ρ, $\mathbf{q}$, P and g are the density, velocity, pressure and gravitational acceleration, respectively. The unit vector $\mathbf{k}$ is in the vertical direction, $\mathbf{\Omega} = \Omega \mathbf{k}$ and the radius vector $\mathbf{r} = x\mathbf{i} + y\mathbf{j}$. If it is assumed that there is static equilibrium, i.e. that the background fluid has no relative motion in the rotating frame of reference, then $\mathbf{q}_e = 0$. A subscript e will be used to denote an equilibrium value and a prime will be used for a disturbance from equilibrium. For equilibrium the momentum equation (3) yields

$$\nabla P_e + \rho_e \mathbf{\Omega} \wedge (\mathbf{\Omega} \wedge \mathbf{r}) + \rho_e g \mathbf{k} = 0. \tag{4}$$

The continuity equation and the linearized momentum equation from (1) and (3) are

$$\nabla . \mathbf{q}' = 0 \tag{5}$$

and
$$\rho_e[\partial \mathbf{q}'/\partial t + 2\mathbf{\Omega} \wedge \mathbf{q}'] = -\nabla P' - \rho' \mathbf{\Omega} \wedge (\mathbf{\Omega} \wedge \mathbf{r}) - \rho' g \mathbf{k}. \tag{6}$$

By taking the curl of the momentum equation (4) it can be shown that

$$\rho_e = \rho_e[z - (\Omega^2 r^2/2g)], \tag{7}$$

where $r^2 = x^2 + y^2$. It will be assumed that $z \gg \Omega^2 r^2/2g$ so that $\rho_e = \rho_e(z)$, i.e the isopycnic surfaces are horizontal. For this case the linearized incompressibility equation (2) becomes

$$\frac{\partial \rho'}{\partial t} + \mathbf{q}' . \left(\frac{d\rho_e}{dz}\mathbf{k}\right) = 0. \tag{8}$$

Two-dimensional waves

The waves will be approximately two-dimensional and parallel to the y axis if the derivatives with respect to y are zero and if the y term in the linearized momentum equation is negligibly small compared with the other terms. This will be the case if $\Omega^2 y \ll g$. The implications of the approximations will be discussed when the theory is compared with experiment.

Let $\mathbf{q}'(x, z) = (u', v', w')$, $u' = \partial\psi/\partial z$ and $w' = -\partial\psi/\partial x$ so that the continuity equation (5) is satisfied. Upon eliminating p', ρ' and v' between (6) and (8) one obtains

$$\frac{\partial^2}{\partial t^2}(\nabla^2\psi) - \frac{N^2}{g}\frac{\partial^3\psi}{\partial z\, \partial t^2} + N^2 \frac{\partial^2 \psi}{\partial x^2} + 4\,\Omega^2 \left(\frac{\partial^2 \psi}{\partial z^2} - \frac{N^2}{g}\frac{\partial \psi}{\partial z}\right) = 0, \tag{9}$$

where N is the buoyancy frequency, $-(g\rho_e^{-1}\, d\rho_e/dz)^{\frac{1}{2}}$.

If we look for a wave solution of the form

$$\psi = \psi_0(z) \exp\{i(k_1 x + k_3 z - \omega t)\}, \tag{10}$$

then (9) can be written as

$$\omega^2\left\{\psi_0\left(k_1^2+k_3^2+i\frac{N^2}{g}k_3\right)+\dot{\psi}_0\left(\frac{N^2}{g}-2ik_3\right)-\ddot{\psi}_0\right\}$$
$$= \psi_0 N^2 k_1^2 + 4\Omega^2\left\{\psi_0\left(k_3^2+i\frac{N^2}{g}k_3\right)+\dot{\psi}_0\left(\frac{N^2}{g}-2ik_3\right)-\ddot{\psi}_0\right\}, \tag{11}$$

where the dot denotes differentiation with respect to z. From the imaginary part of (11), ψ_0 is proportional to $\exp(N^2 z/2g)$, which ensures that energy is conserved. Equation (11) then reduces to the two-dimensional dispersion relation:

$$\omega^2\{k_1^2+k_3^2+(N^2/2g)^2\} = N^2 k_1^2 + 4\Omega^2\{k_3^2+(N^2/2g)^2\}. \tag{12}$$

Three-dimensional waves

If the Boussinesq approximation is applied to (8) and if a wave solution of the form

$$\psi \propto \exp\{i(k_1 x + k_2 y + k_3 z - \omega t)\} \tag{13}$$

is sought, then the three-dimensional dispersion relation takes the form (Rede-kopp 1975)

$$\omega^2(k_1^2+k_2^2+k_3^2) = N^2(k_1^2+k_2^2)+4\Omega^2 k_3^2. \tag{14}$$

By comparing the two-dimensional form of these results with those in the last subsection, it is seen that the Boussinesq approximation implies that

$$(N^2/2g)^2 \ll k_3^2 \quad \text{and} \quad N^2 z/2g \ll 1.$$

The wavenumber direction is defined by the angles ξ and η such that

$$\mathbf{k} = (k_1, k_2, k_3) = |(k_1^2+k_2^2)^{\frac{1}{2}}|\{\cos\xi, \sin\xi, -\tan\eta\}.$$

The dispersion relation (14) can now be written as

$$\omega^2 = N^2\cos^2\eta + 4\Omega^2\sin^2\eta. \tag{15}$$

At sufficiently large distances from the forcing region, the group velocity $\mathbf{c}$ and the phase velocity $\mathbf{v}_p$ are given by (see, for instance, Lighthill 1965) $\mathbf{c} = \nabla_{\mathbf{k}}\omega$ and $\mathbf{v}_p = \omega\mathbf{k}/|\mathbf{k}|^2$. Thus, from the dispersion relation,

$$\mathbf{c} = \frac{(N^2-4\Omega^2)}{\omega|(k_1^2+k_2^2)^{\frac{1}{2}}|}\sin\eta\cos^2\eta\{\sin\eta\cos\xi, \sin\eta\sin\xi, \cos\eta\} \tag{16}$$

and

$$\mathbf{v}_p = \frac{\omega}{|(k_1^2+k_2^2)^{\frac{1}{2}}|}\cos^2\eta\{\cos\xi, \sin\xi, -\tan\eta\}. \tag{17}$$

The theory now follows that of Stevenson (1973). A body starts to move at time t_0 with velocity $\mathbf{Q}(t)$ such that $\mathbf{R}(t)$ is its position with respect to the origin O, which is fixed in the undisturbed background fluid, as in figure 1. The body is at point A at time t_1 and energy radiated from A in a particular direction η reaches

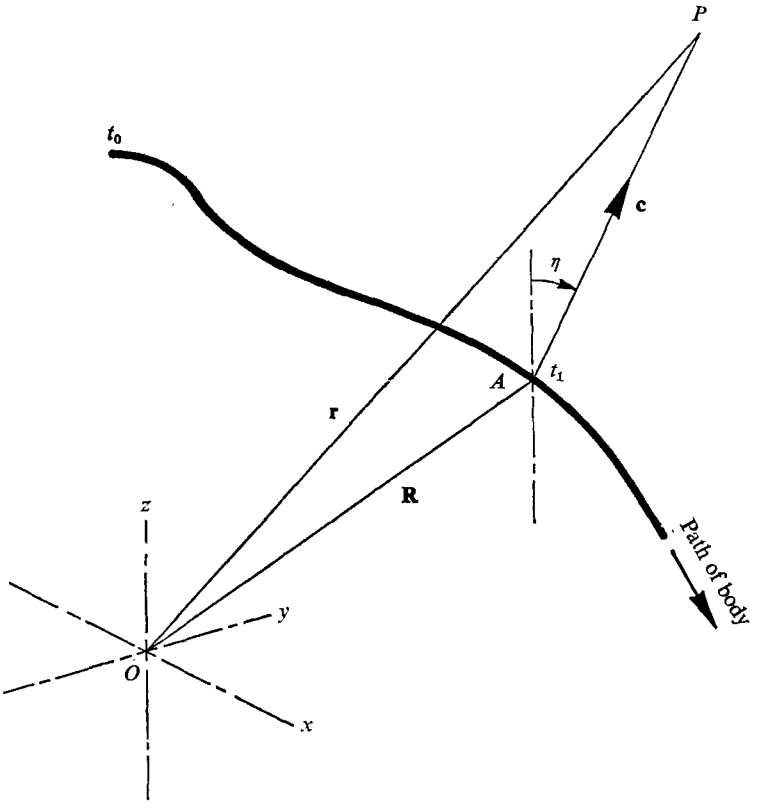

FIGURE 1. The path of the body.

P, at the position $\mathbf{r}(t)$ relative to the origin, at time t. Thus

$$\mathbf{r}(t) = \mathbf{R}_1 + (t - t_1)\,\mathbf{c}, \tag{18}$$

where the subscript one refers to conditions at time $t = t_1$. The phase Φ at P is given by

$$\Phi(t) = (\mathbf{k}.\mathbf{c} - \omega)\,(t - t_1) - \omega_f t_1 + \phi_0, \tag{19}$$

where ω_f is a forcing frequency associated with the body and ϕ_0 is a constant. The relation between ω and ω_f is given by the Doppler equation

$$\omega = \omega_f + \mathbf{Q}_1.\mathbf{k}. \tag{20}$$

As $\mathbf{k}.\mathbf{c} = 0$, (19) implies that

$$t - t_1 = -\phi/(\omega - \omega_f), \tag{21}$$

where $\phi(t) = \Phi(t) - \phi_0 + \omega_f t$. The radiation condition is applied by always ensuring that $t - t_1 > 0$.

If the body moves in the x, z plane such that $\mathbf{Q} = Q(\cos\theta, 0, \sin\theta)$, where θ is the angle which the path of the body makes with the horizontal, then the Doppler equation (20) becomes

$$\omega - \omega_f = Q_1 |(k_1^2 + k_2^2)^{\frac{1}{2}}| \{\cos\theta_1 \cos\xi - \sin\theta_1 \tan\eta\}. \tag{22}$$

The phase configuration is obtained by substituting (16), (21) and (22) into (18), so that

$$\mathbf{r} = \mathbf{R}_1 - \frac{Q_1\phi(N^2-4\Omega^2)}{\omega(\omega-\omega_f)^2}\sin\eta\cos^2\eta\,[\cos\theta_1\cos\xi-\sin\theta_1\tan\eta] \times\{\sin\eta\cos\xi,\ \sin\eta\sin\xi,\ \cos\eta\}. \quad (23)$$

$\phi(t)$ varies by 2π between one wave crest and the next. If the body were a horizontal cylinder then the phase configuration $\mathbf{r}(x,z)$ would be obtained by letting $\xi = 0$ in (23).

When a body moves impulsively, further waves, namely the Cauchy–Poisson waves, are produced. The wavenumbers satisfy the dispersion relation but are not restricted by the Doppler relation. Because $\mathbf{k}.\mathbf{c} = 0$, the phase after a disturbance at time $t = t_0$ is given by

$$\Phi = -\omega(t-t_0). \quad (24)$$

The direction of energy propagation and the lines of constant phase are, from the dispersion relation, inclined to the vertical at an angle η given by

$$\pm[N^2\cos^2\eta+4\Omega^2\sin^2\eta]^{\frac{1}{2}} = \phi/(t-t_0). \quad (25)$$

The wave crests and troughs are vertical circular cones for a point disturbance and St Andrew's crosses for a horizontal line disturbance. When $N > 2\Omega$ the waves appear at the vertical and, as time increases, move towards the horizontal, where they disappear. When $\Omega = 0$ the waves only reach the horizontal when $t = \infty$. If $2\Omega > N$ the waves first appear at the horizontal and move towards the vertical, where they disappear. When $N = 0$ the waves only reach the vertical when $t = \infty$. For all the above cases the number of wave crests increases with time.

3. Comparison of theory with experiment

Apparatus

A glass-sided tank 0·64 m long, 0·23 m high and 50 mm from front to back was filled with stratified brine which had an almost constant buoyancy frequency. The tank was mounted on a rotating table. A schlieren system with 0·3 m diameter mirrors was used to observe the waves which developed when a horizontal circular cylinder of diameter 9 mm was moved through the fluid.

In the theory the following assumptions were made: $\Omega^2r^2/2gz \ll 1$, $\Omega^2y/g \ll 1$, $N^2z/2g \ll 1$ and $N^2/2g \ll k_3$. In the experiments

$$\Omega^2r^2/2gz < 3\times10^{-2}, \quad \Omega^2y/g < 7\times10^{-3}, \quad N^2z/2g < 3\times10^{-2}$$

and

$$N^2/2g \simeq 2\times10^{-4}\,\mathrm{mm}^{-1}.$$

The value of the last of these terms implies that the vertical wavelengths should be very much less than 5 m, which is much larger than the height of the tank.

In a rotating stratified fluid the isopycnic surfaces are not horizontal except on the axis of rotation. The curvature of these surfaces introduces a non-uniform deflexion of the light rays constituting the schlieren beam. This deflexion was found to be negligible compared with that caused by the disturbance.

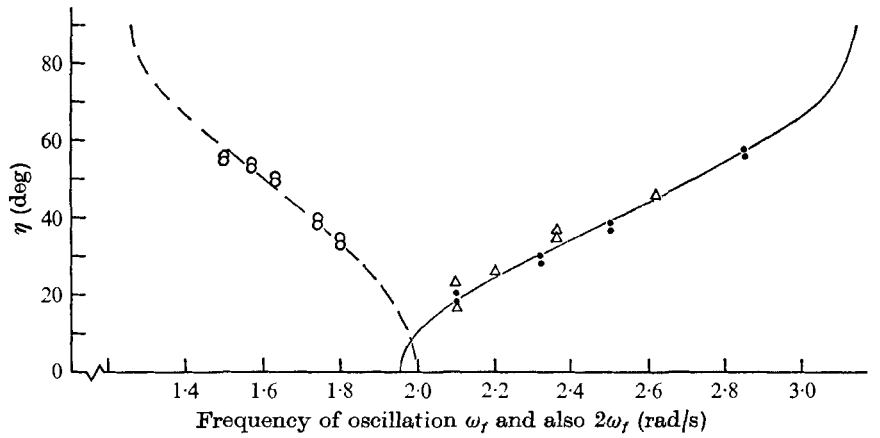

FIGURE 2. An oscillating disturbance. – – – –, equation (15) with $N = 1{\cdot}99$ rad/s, $2\Omega = 1{\cdot}26$ rad/s; ○, experimental points for frequency ω_f; ——, equation (15) with $N = 1{\cdot}95$ rad/s, $2\Omega = 3{\cdot}14$ rad/s; ●, △ experimental points corresponding to ω_f and $2\omega_f$ (second harmonic) respectively.

The experiments were outside the range in which one would expect to find Taylor columns using the criterion giving by Hide & Ibbetson (1966) for purely rotating flow.

An oscillating cylinder

For given ω_f, N and Ω, all the wavenumber vectors are inclined at an angle η to the horizontal. From (16) it follows that the energy propagates at an angle η to the vertical. The lines of constant phase form a St Andrew's cross with arms inclined at η to the vertical. Subba Rao & Prabhakara Rao (1971) considered theoretically the case of an oscillating axisymmetric disturbance and the resultant conical waves have similar angular relationships to those of the crosses considered here.

Primary waves are created when the cylinder's oscillatory frequency ω_f lies between N and 2Ω but higher harmonics will also produce waves if their frequencies lie between N and 2Ω. There are three distinct cases to consider.

(*a*) $N > 2\Omega$. When ω is close to N the arms of the cross-wave are close to the vertical; η is close to 0 or π. As ω decreases towards 2Ω, η tends towards $\frac{1}{2}\pi$ or $\frac{3}{2}\pi$. The phase velocities are directed towards the level of the disturbance.

(*b*) $2\Omega > N$. When ω_f is close to N, η is close to 0 or π. As ω_f increases towards 2Ω, η tends towards $\frac{1}{2}\pi$ or $\frac{3}{2}\pi$. The phase velocities are directed away from the level of the disturbance.

(*c*) When $2\Omega = N$ or when $\omega_f = N$ or $\omega_f = 2\Omega$, the inviscid theory predicts that no waves of finite wavelength exist because the group velocity is zero.

Experimental results showing the relationship between the angle of the waves and the frequency of oscillation are compared with the theory in figure 2. A photograph of one of the crosses is shown in figure 3(*a*) (plate 1).

Cylinder moving with constant velocity

A horizontal cylinder moves with constant velocity at an angle θ to the horizontal, so that $\mathbf{Q}_1 = Q(\cos\theta, \sin\theta)$ and $\mathbf{R}_1 = Qt_1(\cos\theta, \sin\theta)$. Lines of constant phase are

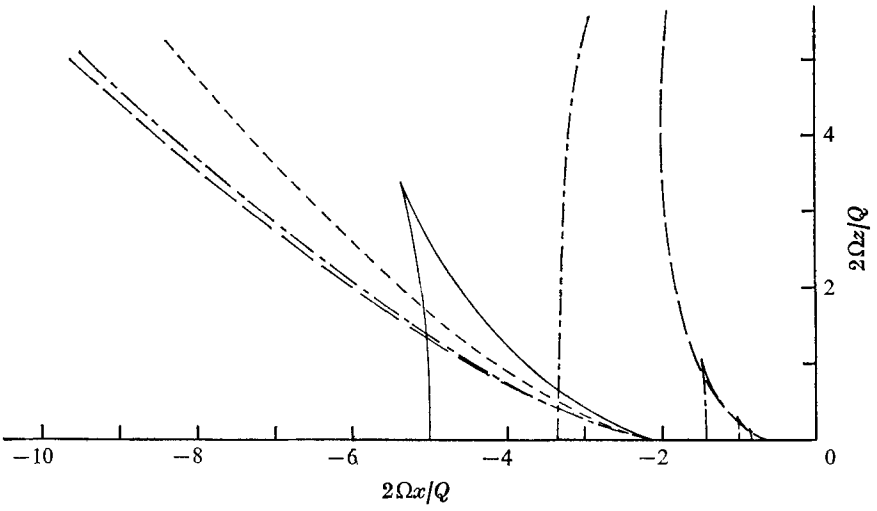

FIGURE 9. Oscillatory wave system with $\omega_f/2\Omega = 0{\cdot}5$, $\theta = 0°$. — — —, $N/2\Omega = 0$; — – —, $N/2\Omega = 0{\cdot}2$; – – – –, $N/2\Omega = 0{\cdot}5$; ——, $N/2\Omega = 0{\cdot}7$.

calculated from (15) and (23) by putting $\xi = 0$. It is useful to note in particular the expressions for $\mathbf{c}$ and $\mathbf{v}_p$:

$$\frac{\mathbf{c}}{Q} = \frac{N^2 - 4\Omega^2}{\omega(\omega - \omega_f)} \sin\eta \cos\eta \cos(\eta + \theta)\{\sin\eta, \cos\eta\}$$

and

$$\frac{\mathbf{v}_p}{Q} = \frac{\omega}{\omega - \omega_f} \cos(\eta + \theta)\{\cos\eta, -\sin\eta\},$$

with

$$\omega^2 = N^2 \cos^2\eta + 4\Omega^2 \sin^2\eta.$$

(*a*) *The case* $\omega_f = 0$. When both N and Ω are non-zero, the group velocity never tends to infinity for any combination of η and θ. Thus the waves are always of finite extent, as distinct from those in a solely rotating or solely stratified fluid. Furthermore as $|N^2 - 4\Omega^2| \to 0$ the wave region becomes smaller in extent and in the limit the energy is confined to the path of the body. The wave system relative to a body moving at an angle θ in a fluid where $N > 2\Omega$ is similar to that generated by a body moving at an angle of $\theta \pm \frac{1}{2}\pi$ in a fluid with $2\Omega > N$.

The characteristics of the waves are demonstrated in figures 3(*b*)–(*d*), 4, 5 and 6(*a*) (plates 1–4). The theoretical phase configurations have been computed for equal increments of η. Points very close together have been joined. The experiments compare quite well except where the wake interferes with the wave system.

Theoretically each line of constant phase intersects the path of the body twice. One family of intersections are $2\pi Q/N$ apart, which is also the wave spacing when $\Omega = 0$. The other intersections are $\pi Q/\Omega$ apart, which is the same as that when $N = 0$.

Impulsive-start waves have the same phase as, and are tangential to, any incomplete waves of the steady wave system, as in the purely stratified case (Stevenson 1973).

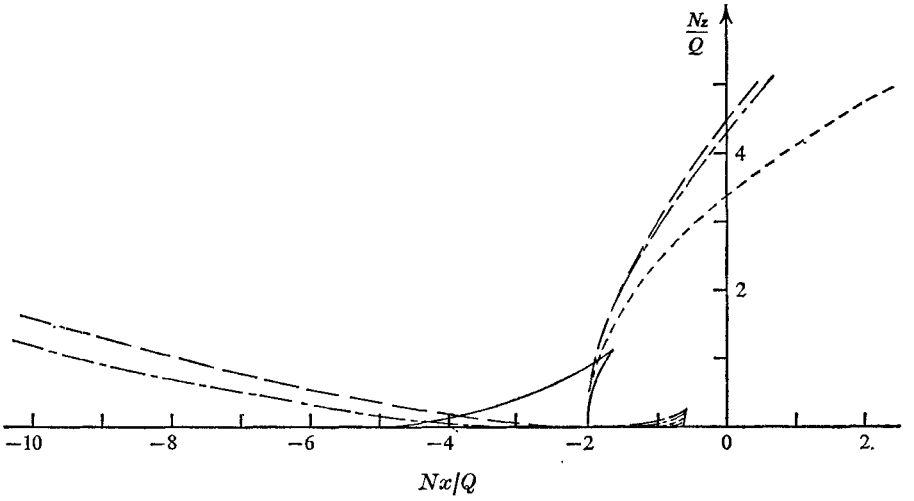

FIGURE 10. Oscillatory wave system with $\omega_f/N = 0{\cdot}5$, $\theta = 0$. — — —, $2\Omega/N = 0$; — - —, $2\Omega/N = 0{\cdot}2$; - - - -, $2\Omega/N = 0{\cdot}5$; ——, $2\Omega/N = 0{\cdot}7$.

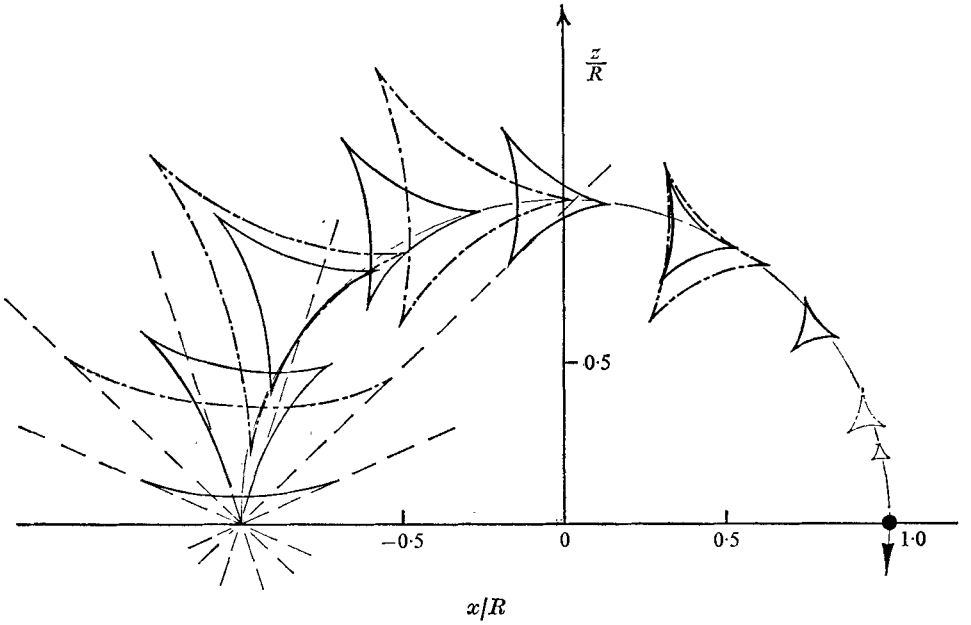

FIGURE 11. Oscillatory wave system when the body moves in a circular path. $\omega_c t_0 = 0$, $\omega_c t = \pi$, $N/\omega_c = 10{\cdot}2$, $2\Omega/\omega_c = 12{\cdot}8$, $\omega_f/\omega_c = 2{\cdot}55$. — — —, impulsive-start waves.

(*b*) *The case* $\omega_f \neq 0$. When ω_f is less than both N and 2Ω or when ω_f is greater than both N and 2Ω, the group velocity is always finite and for each value of ϕ there are two closed waves: waves in which the crests and troughs do not stretch to infinity. When ω_f is between N and 2Ω there is, for each ϕ, one closed wave and one wave whose two arms stretch towards infinity. For other values of ω_f there are no closed waves. Obviously, incomplete waves will exist which are associated with the impulsive start.

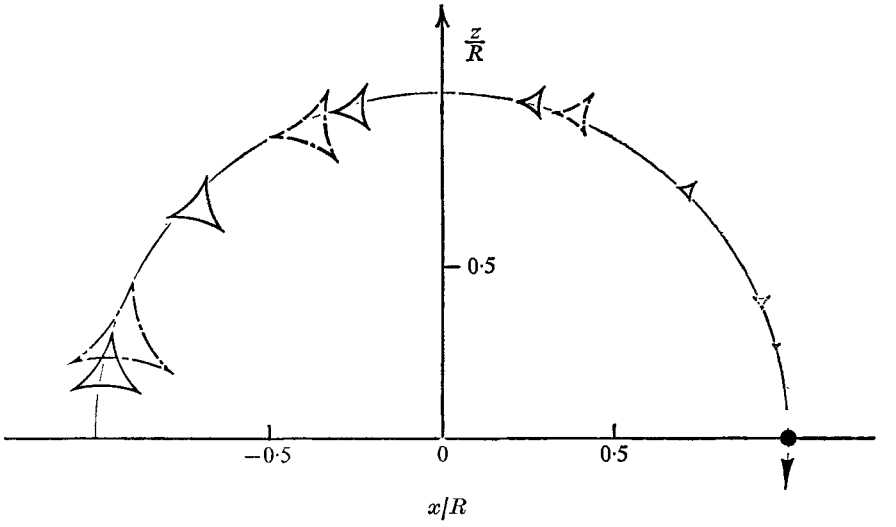

FIGURE 12. Oscillatory wave system when the body moves in a circular path. $\omega_c t_0 = 0$, $\omega_c t = \pi$, $N/\omega_c = 10{\cdot}2$, $2\Omega/\omega_c = 9{\cdot}6$, $\omega_f/\omega_c = 1{\cdot}8$.

Examples of the phase configuration are shown in figures 9 and 10. There is more detail in these figures than in those given by Redekopp (1975).

Cylinder moving in a circular path

A cylinder at $(-R, 0)$ starts from rest and travels in a circular path of radius R with a constant angular frequency ω_c, such that $\omega_c R = Q$. Then

$$\mathbf{R}_1 = R(-\cos\omega_c t_1, \sin\omega_c t_1) \quad \text{and} \quad \mathbf{Q}_1 = Q(\sin\omega_c t_1, \cos\omega_c t_1).$$

Lines of constant phase are found from (23) by letting $\psi = 0$.

The general characteristics of the wave patterns are the same as those in the previous subsection. The theory and experiments with $\omega_f = 0$ are compared in figures 6(*b*), 6(*c*), 7 and 8 (plates 4–6). For simplicity the theoretical waves corresponding to large ϕ are not presented in the figures. These waves, which correspond to energy which has been propagating for the longest time, are not visible in the schlieren photographs, presumably because of viscous effects. In the experiments large regions of the wave patterns are obliterated by the wide wakes.

Examples when ω_f is not zero are given in figures 11 and 12 and illustrate how waves produced when a body is moving at an angle θ in a fluid with $N > 2\Omega$ are of a similar shape to those at $\theta + \frac{1}{2}\pi$ in a fluid with $2\Omega > N$. They also illustrate how the wave system decreases in size as $|N - 2\Omega| \to 0$. Impulsive-start waves are included where they are present, which is in figure 11 only.

4. Conclusions

Equations have been derived to determine the phase configuration of the waves which develop around a body moving on an arbitrary path in a rotating stratified

fluid. The wave patterns have been calculated using the radiation condition during the computation and the wavenumber surfaces have not been used explicitly. Solutions have been obtained for bodies in steady motion and for bodies with a superimposed forcing frequency. Experiments have been conducted using a cylinder moving steadily in a rotating tank of stratified brine. The waves generated, viewed by a schlieren system, agree quite well with the theoretical phase configurations.

The authors appreciate the helpful discussions with Professor N. H. Johannesen. The work was supported by the Procurement Executive, Ministry of Defence. K. S. Peat was in receipt of a Science Research Council Maintenance Grant.

REFERENCES

GÖRTLER, H. 1943 *Z. angew. Math. Mech.* **23**, 65.
GÖRTLER, H. 1944 *Z. angew. Math. Mech.* **24**, 210.
GÖRTLER, H. 1957 *5th Midwestern Conf. Fluid Mech., Univ. Michigan*, pp. 1–10.
GREENSPAN, H. P. 1968 *The Theory of Rotating Fluids*. Cambridge University Press.
HIDE, R. & IBBETSON, A. 1966 *Icarus*, **5**, 279.
LIGHTHILL, M. J. 1965 *J. Inst. Math. Appl.* **1**, 1.
LIGHTHILL, M. J. 1967 *J. Fluid Mech.* **27**, 725.
MOWBRAY, D. E. & RARITY, B. S. H. 1967 *J. Fluid Mech.* **28**, 1.
NIGAM, S. D. & NIGAM, P. D. 1962 *Proc. Roy. Soc.* A **266, 247.**
OSER, H. 1958 *Z. angew. Math. Mech.* **38**, 386.
PRABHAKARA RAO, G. V. 1973 *J. Fluid Mech.* **61**, 129.
RARITY, B. S. H. 1967 *J. Fluid Mech.* **30**, 329.
REDEKOPP, L. G. 1975 *Geophys. Fluid Dyn.* **6**, 289.
STEVENSON, T. N. 1969 *J. Fluid Mech.* **35**, 219.
STEVENSON, T. N. 1973 *J. Fluid Mech.* **60**, 759.
STEVENSON, T. N. & THOMAS, N. H. 1969 *J. Fluid Mech.* **36**, 505.
SUBBA RAO, V. & PRABHAKARA RAO, G. V. 1971 *J. Fluid Mech.* **46**, 447.

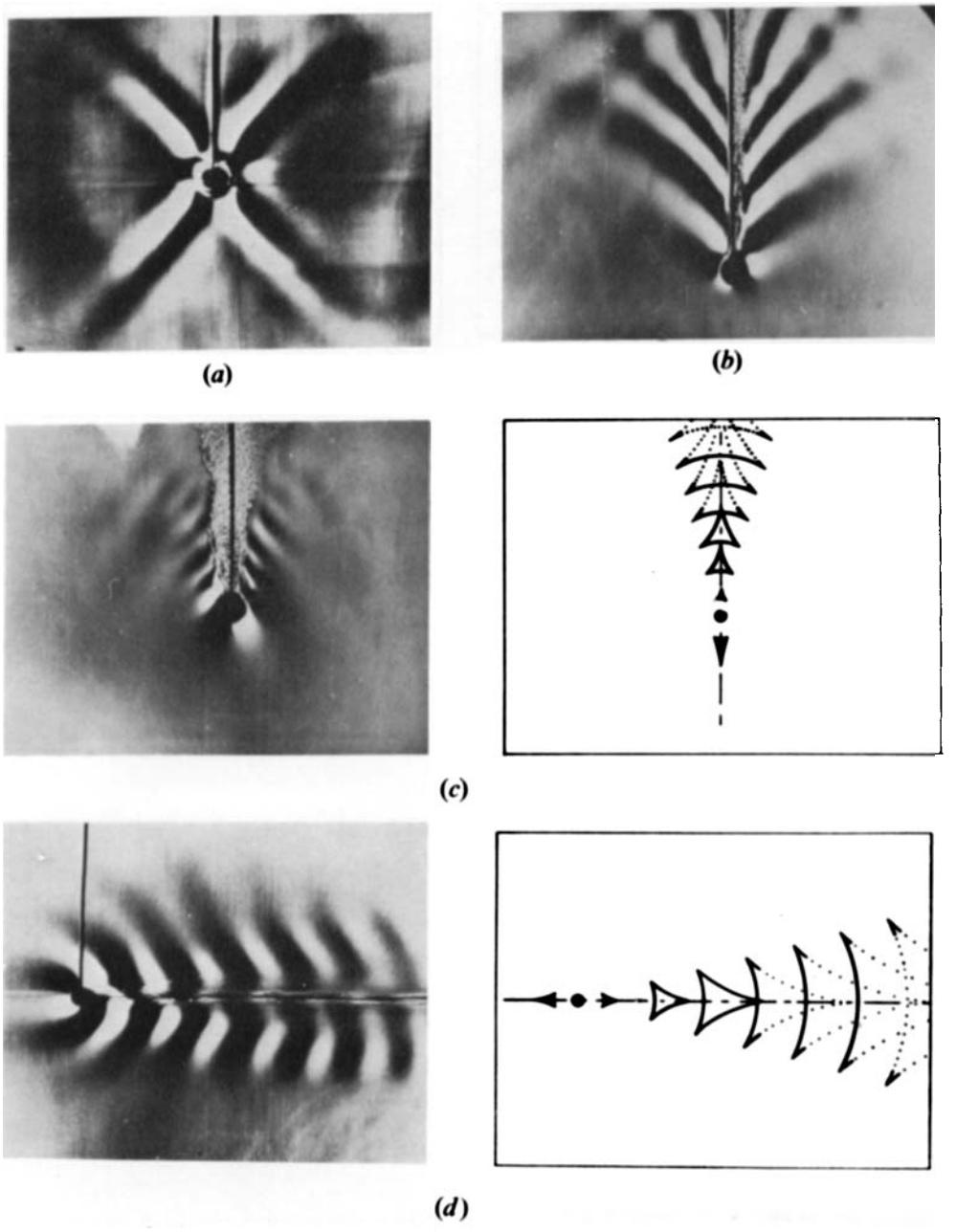

FIGURE 3. (*a*) Oscillating disturbance, $\omega_f = 2{\cdot}70$ rad/s, $N = 2{\cdot}32$ rad/s, $2\Omega = 3{\cdot}14$ rad/s. (*b*), (*c*) Cylinder moving vertically, $Q = 7{\cdot}3$ mm/s, $N = 1{\cdot}94$ rad/s, $\omega_f = 0$. (*b*) $2\Omega = 0$; (*c*) $2\Omega = 3{\cdot}14$ rad/s. (*d*) Cylinder moving horizontally, $Q = 8{\cdot}0$ mm/s, $N = 1{\cdot}94$ rad/s, $2\Omega = 1{\cdot}26$ rad/s.

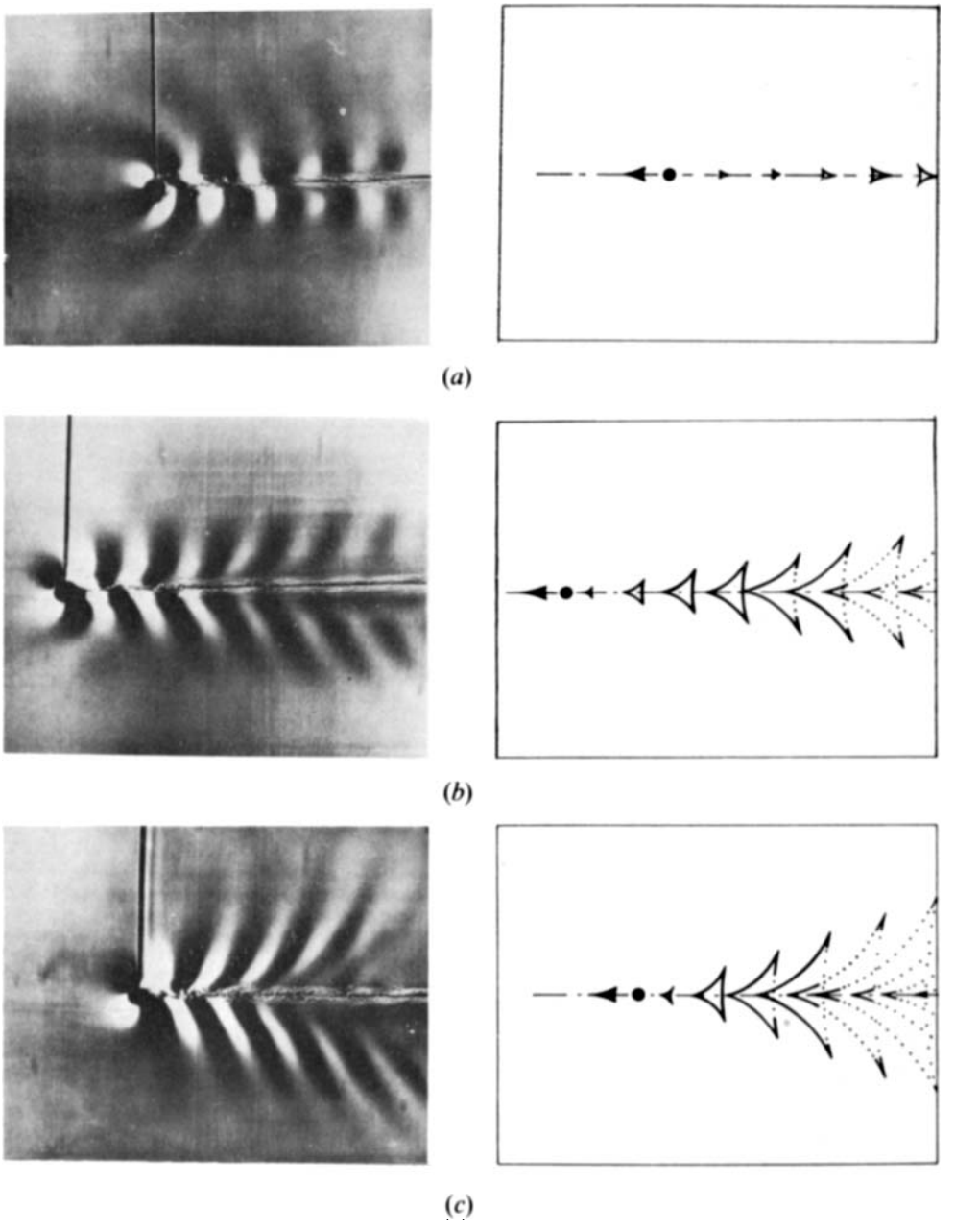

FIGURE 4. Cylinder moving horizontally, $Q = 8{\cdot}0$ mm/s, $N = 1{\cdot}94$ rad/s.
(*a*) $2\Omega = 1{\cdot}88$ rad/s; (*b*) $2\Omega = 2{\cdot}51$ rad/s; (*c*) $2\Omega = 3{\cdot}14$ rad/s.

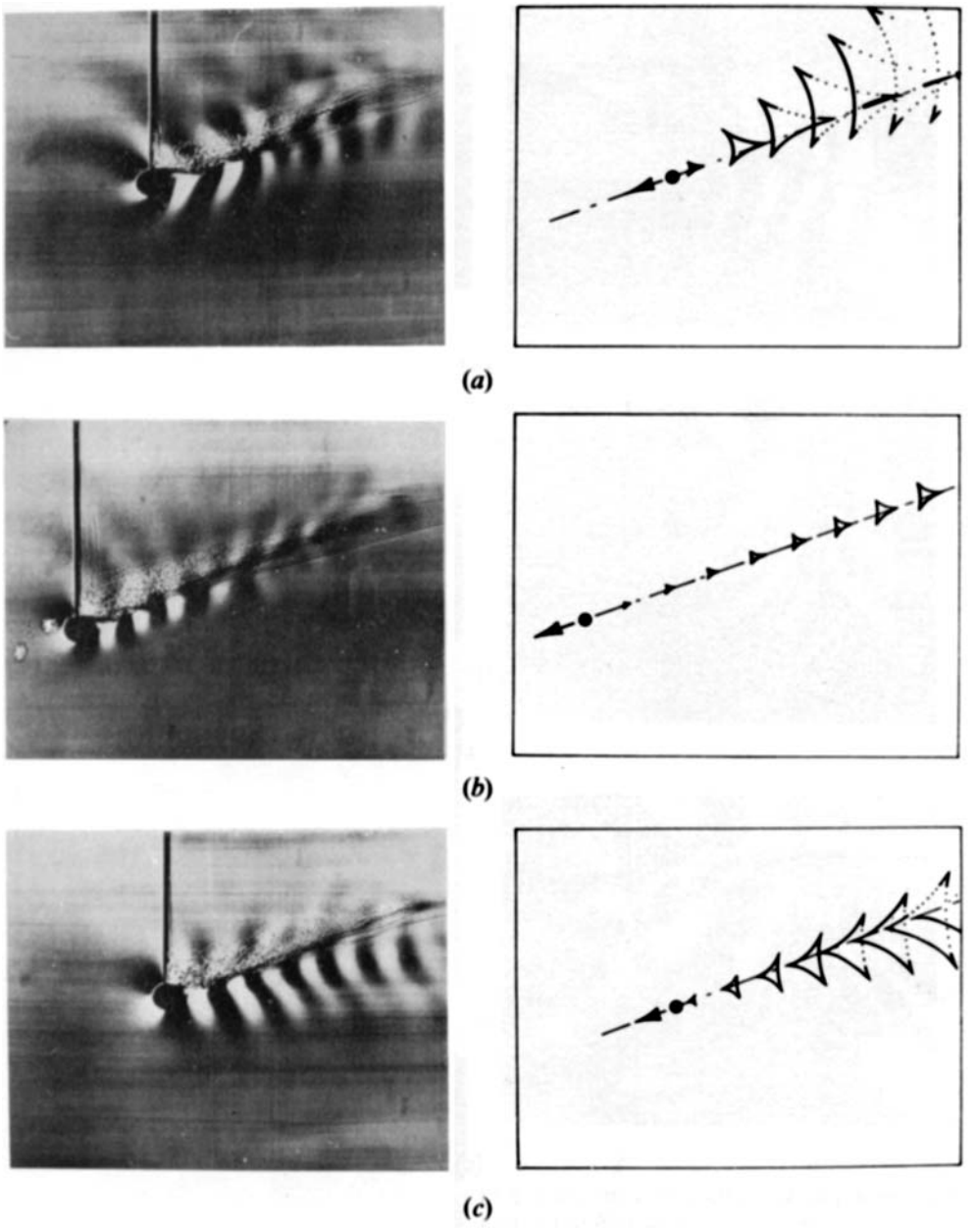

FIGURE 5. Steady wave systems when $\theta = 20°$, $Q = 8$ mm/s, $N = 1{\cdot}94$ rad/s. (*a*) $2\Omega = 1{\cdot}26$ rad/s; (*b*) $2\Omega = 1{\cdot}88$ rad/s; (*c*) $2\Omega = 2{\cdot}51$ rad/s.

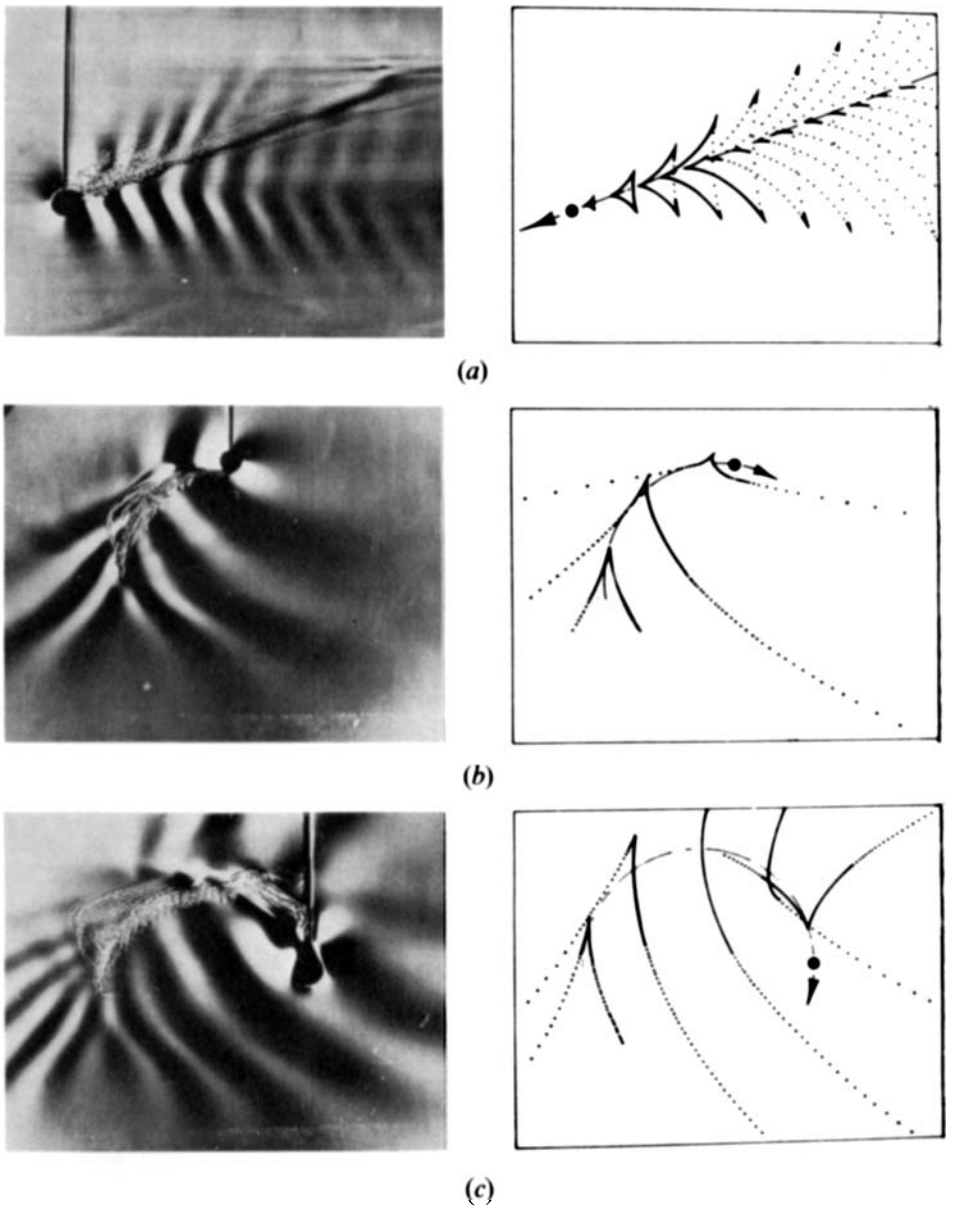

FIGURE 6. (*a*) As for figure 5 with $2\Omega = 3{\cdot}14$ rad/s. (*b*), (*c*) Circular path of radius 60 mm, $\omega_c = 0{\cdot}29$ rad/s, $N = 1{\cdot}99$ rad/s, $\Omega = 0$, $\omega_c t_0 = 0$. (*b*) $t = 9$ s; (*c*) $t = 24$ s.

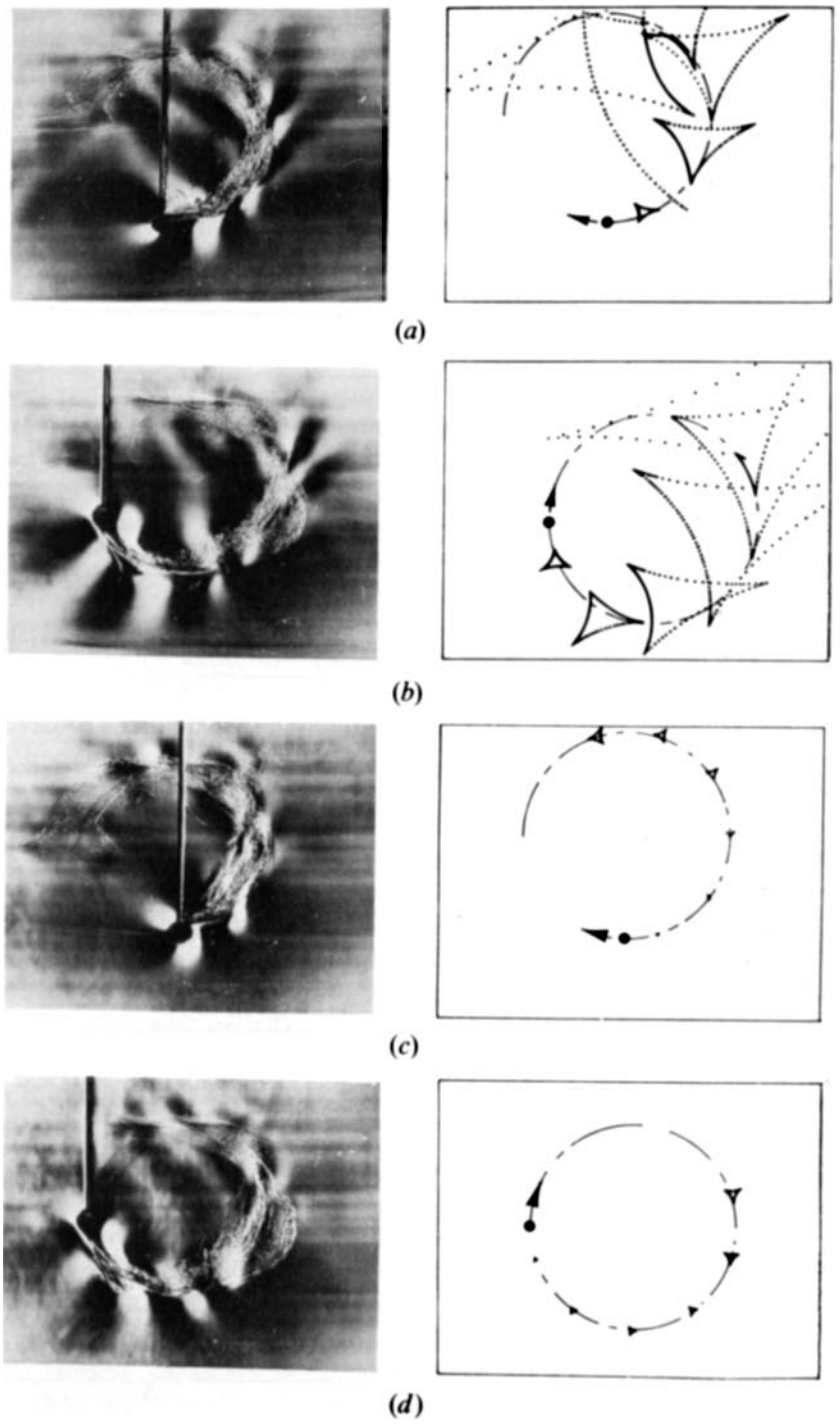

FIGURE 7. Circular path, $R = 60$ mm, $N = 1{\cdot}99$ rad/s, $\omega_c = 0{\cdot}20$ rad/s. (*a*), (*b*) $2\Omega = 1{\cdot}26$ rad/s, and $t = 24$ s and 32 s respectively. (*c*), (*d*) $2\Omega = 1{\cdot}88$ rad/s, and $t = 24$ s and 32 s respectively.

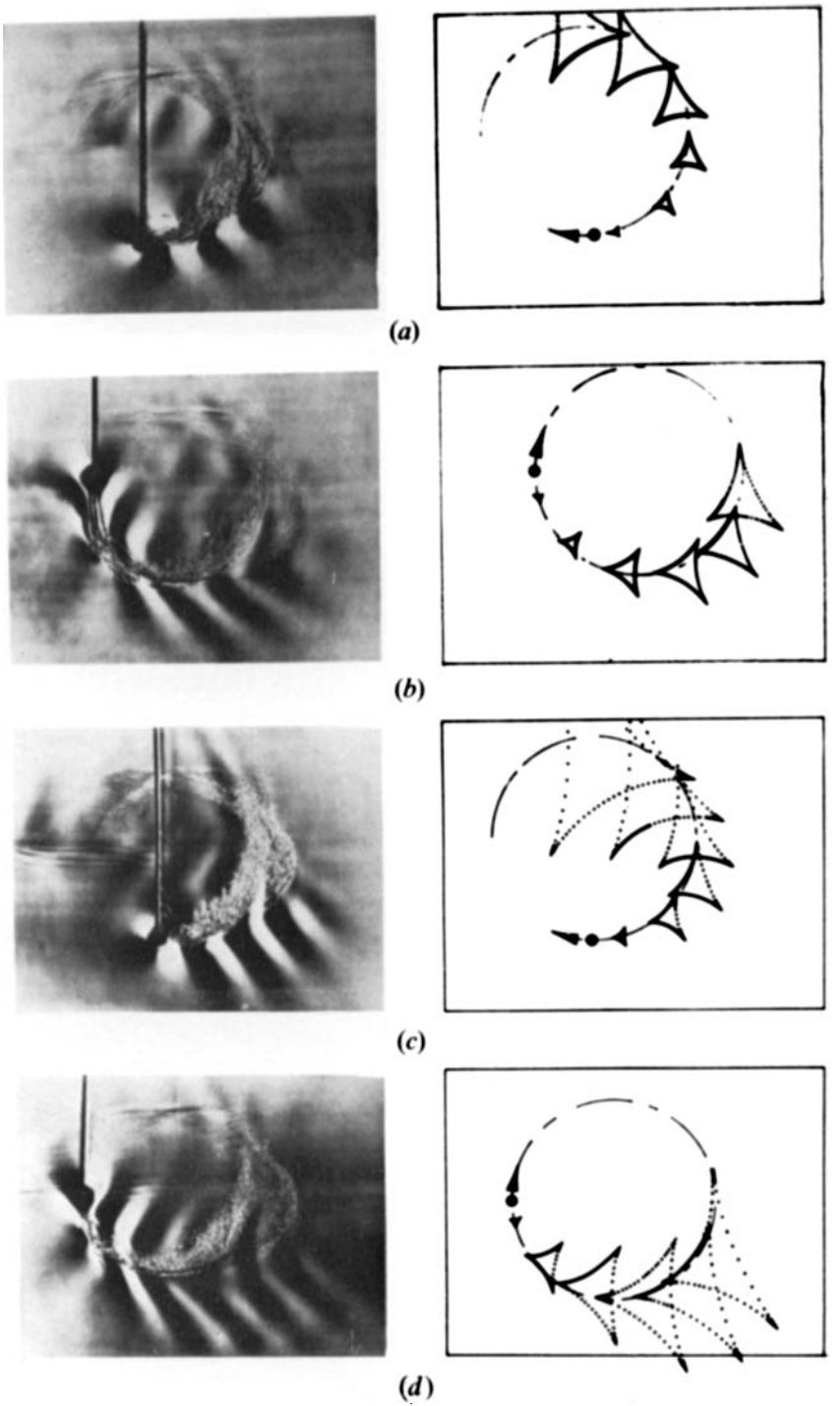

FIGURE 8. Circular path, $R = 60$ mm, $N = 1{\cdot}99$ rad/s, $\omega_c = 0{\cdot}20$ rad/s. (*a*), (*b*) $2\Omega = 2{\cdot}51$ rad/s, and $t = 24$ s and 32 s respectively. (*c*), (*d*) $2\Omega = 3{\cdot}14$ rad/s, and $t = 24$ s and 32 s respectively.